PAPER • OPEN ACCESS

Characterisation of the UK high energy proton research beamline for high and ultra-high dose rate (FLASH) irradiation

To cite this article: J D Aylward *et al* 2023 *Biomed. Phys. Eng. Express* **9** 055032

Biomedical Physics & Engineering Express

CrossMark

OPEN ACCESS

RECEIVED
19 July 2023

REVISED
2 August 2023

ACCEPTED FOR PUBLICATION
11 August 2023

PUBLISHED
4 September 2023

PAPER

Characterisation of the UK high energy proton research beamline for high and ultra-high dose rate (FLASH) irradiation

J D Aylward[1,2,3], N Henthorn[1,4], S Manger[1,4], J W Warmenhoven[1,4], M J Merchant[1,4], M J Taylor[1,3,4], R I Mackay[1,2] and K J Kirkby[1,3,4]

[1] Division of Cancer Sciences, Faculty of Biology, Medicine and Health, The University of Manchester, Manchester, United Kingdom
[2] Christie Medical Physics and Engineering, The Christie NHS Foundation Trust, Manchester, United Kingdom
[3] Cockcroft Institute, Daresbury Laboratory, Keckwick Ln, Daresbury, Warrington WA4 4AD, United Kingdom
[4] The Christie NHS Foundation Trust, Manchester, United Kingdom

E-mail: jack.aylward@postgrad.manchester.ac.uk

Keywords: ultra-high dose rate (UHDR), proton, dosimetry, FLASH

Abstract

Objective. This work sets out the capabilities of the high energy proton research beamline developed in the Christie proton therapy centre for Ultra-High Dose Rate (UHDR) irradiation and FLASH experiments. It also characterises the lower limits of UHDR operation for this Pencil Beam Scanning (PBS) proton hardware. *Approach.* Energy dependent nozzle transmission was measured using a Faraday Cup beam collector. Spot size was measured at the reference plane using a 2D scintillation detector. Integrated depth doses (IDDs) were measured. EBT3 Gafchromic film was used to compare UHDR and conventional dose rate spots. Our beam monitor calibration methodolgy for UHDR is described. A microDiamond detector was used to determine dose rates at z_{ref}. Instantaneous depth dose rates were calculated for 70–245 MeV. PBS dose rate distributions were calculated using Folkerts and Van der Water definitions. *Main results.* Transmission of $7.05 \pm 0.1\%$ is achieveable corresponding to a peak instantaneous dose rate of 112.7 Gy s^{-1}. Beam parameters are comparable in conventional and UHDR mode with a spot size of $\sigma_x = 4.6$ mm, $\sigma_y = 6.6$ mm. Dead time in the beam monitoring electonics warrants a beam current dependent MU correction in the present configuration. Fast beam scanning of 26.4 m s^{-1} (X) and 12.1 m s^{-1} (Y) allows PBS dose rates of the order tens of Grays per second. *Significance.* UHDR delivery is possible for small field sizes and high energies enabling research into the FLASH effect with PBS protons at our facility. To our knowledge this is also the first thorough characterisation of UHDR irradiation using the hardware of this clinical accelerator at energies less than 250 MeV. The data set out in this publication can be used for designing experiments at this UK research facility and inform the possible future clinical translation of UHDR PBS proton therapy.

1. Introduction

The UK's first NHS high energy proton radiotherapy facility opened in 2019 at The Christie's Withington site in Manchester. The facility comprises three clinical treatment rooms and a 4th room—the Stoller Research Room—operated by the University of Manchester's PRECISE group which is not used for clinical treatment. The research room has a bespoke experimental beam line for proton biology and technical research. This paper explores the development of an Ultra-High Dose Rate (UHDR) capability for FLASH and UHDR dosimetry research.

Interest in UHDR has recently been reignited due to the so called 'FLASH effect' [1, 2], with FLASH being voted the 'hottest' topic in Radiation Oncology at the American Society for Radiation Oncology (ASTRO) conference in 2021. The effect has been characterised experimentally by a reduction in normal tissue complication with conserved tumour control [3]. Independent of the FLASH effect, UHDR dosimetry has become a research field in its own right [4], and faster radiotherapy using UHDR has potential clinical benefits including reduced intrafraction motion as well as reduced treatment delivery time which may result in higher patient throughput. These

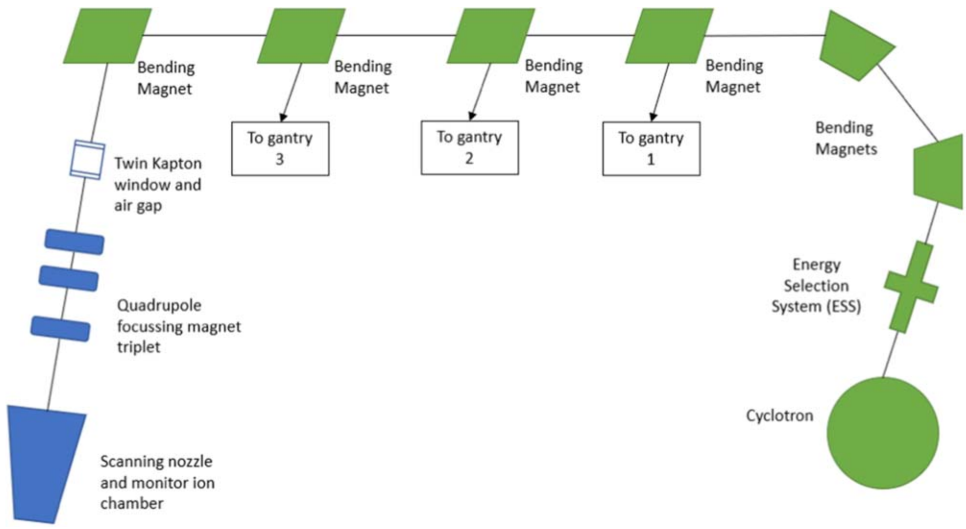

Figure 1. Schematic diagram of the beamline showing relevant components for this publication for clarity. Beamline A is shown in blue with the clinical section of the beamline in green.

benefits are possible without any particular dose rate being required. UHDR research focusing on dosimetry is needed to accelerate the translation of higher dose rate radiotherapy into clinical use.

The Research Room can deliver UHDR proton beams via a fixed horizontal beamline (Beamline A) designed for *in vitro* research. Designs are being developed for a second beamline (Beamline B) to extend the research capabilities. Beamline A in our facility is commissioned to deliver a beam at the maximum cyclotron current for any energy in the standard clinical configuration for this accelerator of 70–245 MeV. Other facilities using our accelerator hardware have generally only used 250 MeV for UHDR and FLASH experiments, whereas we have the capability to deliver and investigate the use of UHDR at lower energies across the full clinical energy range. We believe we are the first to investigate and report on the maximum dose rates available at all the available energies. This expands the explored parameter space for this system which is ultimately required prior to any clinical translation of UHDR.

At our facility the maximum proton transmission from the cyclotron to the research room nozzle is at 245 MeV (rather than 250 MeV). The equipment vendor cites the multi-vendor configuration of our research room as a reason for this. All aspects of the beamline capabilities into the research room (energy, transmission, proton beam current, spot size) are determined by the vendor who controls the functionality and beam from the cyclotron to the twin Kapton window interface between the clinical section of the beamline and the research room (figure 1). We understand that other institutions may be in a similar situation, having a maximum transmission and energy of 245 MeV. This increases the relevance of this work to the community: understanding the dose rates that are achievable in the standard configuration of 70–245 MeV has become highly relevant to those carrying out research using UHDR and High Dose Rate (HDR) beams.

The Manchester beamline is an international facility for proton research and can be accessed via EU (INSPIRE, canSERV) and CRUK (RadNet and FLASH infrastructure). This paper characterises the beamline and sets out the commissioning results, focusing on UHDR capabilities. It is the first paper to detail UHDR irradiations with this hardware using energies less than 250 MeV. The paper also presents the parameters required to describe the Manchester beamline for any UHDR experimental work.

2. Method

2.1. Beam characterisation

Beamline A is supplied by a 250 MeV ProBeam isochronous cyclotron (Varian Medical Systems, Palo Alto, CA), operating at 72 MHz (0.4 ns proton bunches with 13.9 ns repetition time). Proton currents of up to 800 nA can be requested from the cyclotron [3]. Energies lower than 250 MeV are obtained by degrading the beam using a double-carbon wedge energy selection system (ESS) combined with a collimator assembly used to maintain a circular spot. The ESS results in an energy dependent beam transmission to the nozzle. The research room beamline (figure 1) is isolated from the clinical beamline by a twin Kapton window (125 μm each) and air gap between the windows of 100 mm.

Inside the Research Room, Beamline A comprises a quadrupole magnet triplet, two retractable beam profile monitors, and the hardware from a ProBeam gantry nozzle in a fixed horizontal orientation. The nozzle comprises orthogonal scanning magnets to enable Pencil Beam Scanning (PBS), and a Multi-Strip Ionisation Chamber (MSIC) with a Pyramid IC101 electrometer used for beam monitoring. A geometrical reference plane has been defined at 2560 mm and 2000 mm from the Y- and X- scanning magnets respectively and is aligned with the centre of the nozzle. The beam is aligned to this reference plane. Pillar mounted APOLLO green LAP lasers (Lap Laser Applications LLC, Lüneburg, Germany) are used to aid positioning of equipment. Beam optics along the beamline have been optimised using TRANSPORT [5].

A scanned area of up to 40 × 30 cm is achievable at the reference plane, with larger scan areas being possible at a greater distance from the nozzle. Beam scanning speeds of up to 26.4 m s^{-1} horizontally (X) and 12.1 m s^{-1} vertically (Y) at reference plane can be achieved. Two scanning modes are available: Discrete and continuous. For discrete mode the beam is terminated between the delivery of each spot, whereas it remains on in continuous mode. An interlocked water tank is currently used as a beamstop, and a permanent water based beamstop will be bought into use in 2023. Control of the Research Room beamline is via bespoke software which interfaces with the cyclotron via the Varian Racehorse system.

The beam spot size was determined in water using a PTW MP3-M Water Phantom with microDiamond detector type 60019 (PTW, Freiburg), and in air using the IBA LYNX scintillation detector (Ion Beam Applications, Belgium). The linearity of the microDiamond response with beam current was verified prior to being used for measurements. The LYNX detector has previously been used in PBS proton beams of these dose rates [6]. EBT3 Gafchromic film was used to compare 245 MeV spots delivered at conventional and ultra-high dose rates. A red channel calibration created at conventional dose rates was applied to both films.

Integrated Depth Dose (IDD) measurements were obtained in water at conventional dose rates (up to 2 nA nozzle current) using a PTW MP3-M Water Phantom and a PTW Bragg Peak Chamber Type 34070. A PTW Thin Window Bragg Peak Chamber Type 34080 was used as a reference detector. Proton Ranges (R_{80}) were determined and a fit calculated as per the methods set out in Bortfield *et al* [7, 8].

Percentage transmission from the cyclotron to the nozzle was measured using a Pyramid BC-75 Solid Core Faraday Cup (Pyramid Technical Consultants Inc., Waltham MA, USA) aligned to the reference plane. A Pyramid F460 4-Channel Precision Electrometer was used. The dimensions of the BC-75 are sufficient to collect > 99.9% of the beam at 245 MeV. The transmission along the beamline was determined as a function of energy, from 70–245 MeV, using 800 nA requested cyclotron current. The variation in transmission was also measured across the nozzle current range, from 1.35–56.4 nA, for 245 MeV. Uncertainties in transmission were determined using standard propagation of error.

Conventional and UHDR spot profiles were measured in water at z_{ref} using EBT3 Gafchormic film and normalised to give relative dose and dose rate distributions to determine any change in spot size or shape when operating at UHDR compared to conventional dose rates.

PBS proton experiments are forward-planned using a correction based dose calculation to create square or rectangular spot maps of a uniform dose. Eclipse V15.1 is also available for planning. EBT3 Gafchromic film is routinely used, scanned with an EPSON Expression 12000XL, for *in vitro* absolute dose verification as well as beam alignment checks. EBT3 film has been demonstrated to be a dose rate independent detector for UHDR protons across this dose rate range and beam quality [9, 10].

2.2. Absolute dose determination

The integral plane of the monitor ion chamber is used to control the dose of the UHDR beam. Positional information from the MSIC is not routinely used. A bias of +1200 V was applied to channel 1 of the two integral plane ion chambers and the signal recorded using an IC101 electrometer sampling at 9.009 kHz. The monitor chamber current was assessed for the range of available nozzle currents (up to 56.4 nA) to determine the extent of ion recombination within the chamber volume.

The MSIC and electrometer system is designed for conventional dose rates (nozzle current up to 2 nA). When used for UHDR a significant Monitor Unit (MU) correction is required to account for signal losses due to ion recombination and to account for any dead time in the electronics.

'UHDR beam' in this manuscript refers to a beam at the maximum energy and cyclotron current: This is 245 MeV and 800 nA for our beamline at this time. The MU correction was carried out for a UHDR beam based on TRS398 [11] reference conditions, with a 5 × 5 cm square field and a reference depth, z_{ref}, of 2 cm. A rectangular raster scanning pattern was used with 2.5 mm spot separation and the beam running in continuous mode. A PTW Advanced Markus Type 34045 ionisation chamber traceable to the National Physical Laboratory (NPL, Teddington, UK) primary standard was used for absolute dose determination in water at conventional and UHDR. A PTW Unidos E electrometer was used. The two-voltage method was used [12] to account for ion recombination in the Advanced Markus and a correction factor, k_s, determined as has been used elsewhere for a quasi-continuous beam proton beam of this dose rate [10]. A beam current dependent MU scaling factor was determined as per equation (1) where $MU_{UHDR,D}$ and $MU_{CONV,D}$ are the MU required to deliver a dose, D, at UHDR and conventional dose rates respectively. $R_{CONV,D}$ $R_{UHDR,D}$ and $R_{UHDR,0MU}$ are the detector readings, in nC, for a conventional, UHDR, and 0 MU beam running in continuous mode, respectively.

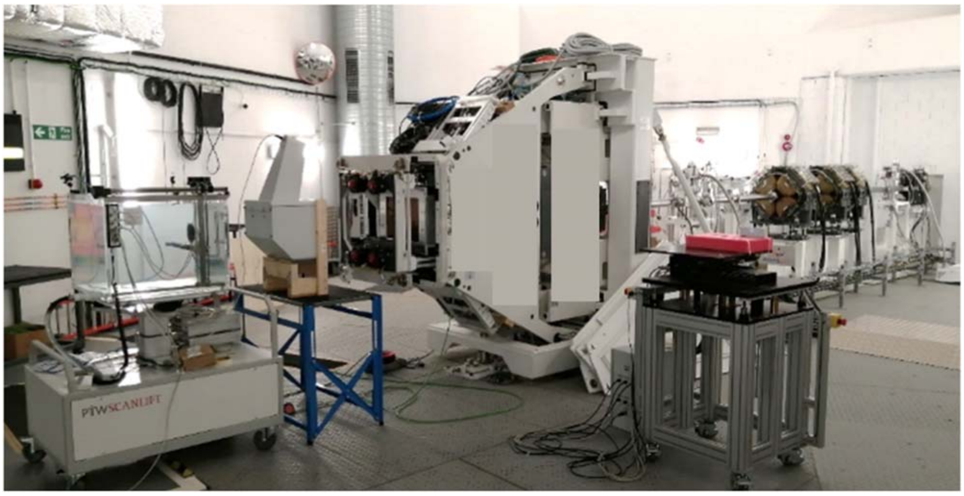

Figure 2. Photograph of Beamline A with PTW water tank and IBA LYNX detector positioned at the reference plane.

$$MU_{UHDR,\,D} = MU_{CONV,\,D}\left[\frac{(R_{CONV,\,D} - R_{UHDR,\,0\,MU})}{R_{UHDR,\,D}}\right] \quad (1)$$

This UHDR MU correction was determined across the range of possible nozzle currents. An alternative and practical method for monitor chamber calibration is to iteratively adjust the MU until the required dose is obtained when measured under our UHDR reference conditions. Both of these methods are subject to a beam current dependent variation in required correction. An ion recombination correction, k_s, was also determined for the PTW Roos in combination with the Unidos E.

2.3. Dose rate determination

Peak instantaneous spot dose rates (centre of gaussian spot) were measured in water as a function of cyclotron current for 245 MeV at the reference depth using the PTW microDiamond and Unidos E electrometer operating in *High* range. The detector was aligned to the centre of the spot profile at the reference plane at 2 cm depth. The dose rate recorded was an average across the 3.8 mm^2 area of the sensitive area of the detector, and was determined from the Unidos measured current and microDiamond calibration factor. This calibration was carried out using conventional dose rates against a PTW Roos secondary standard traceable to the National Physical Laboratory primary standard.

Calculated central axis (CAX) depth doses were scaled by the measured dose rate and transmission to give a central axis dose rate profile in water for 70, 150, 230, and 245 MeV spots. PBS proton dose rate distributions for a UHDR transmission beam are created for UHDR experiments using both the Dose Averaged Dose Rate (DADR) [13] (which does not account for the temporal separation of spots) and Averaged Dose Rate (ADR, also known as 'PBS Dose Rate', which does account for the temporal separation of spots) [14].

For ADR the dose rate, $\dot{D}_j$, to the j^{th} voxel or pixel is given by equation (2) where D_j is the total dose delivered to a voxel, and T_j is the time for the dose to be delivered to the j^{th} voxel between lower and upper dose thresholds, d.

$$\dot{D}_j^{ADR} = \frac{D_j - 2d}{T_j} \quad (2)$$

For DADR the dose rate to the j^{th} voxel or pixel is given by equation (3) where $D_{j,i}$ is the dose to the j^{th} voxel from the i^{th} spot, $\dot{D}_{j,i}$ is the dose rate to the j^{th} voxel from the i^{th} spot, and N is the total number of spots.

$$\dot{D}_j^{DADR} = \sum_{i=1}^{N} \frac{D_{j,i}}{\sum_{i=1}^{N} D_{j,i}} \dot{D}_{j,i} \quad (3)$$

Examples of DADR and ADR distributions are given for a 5 × 5 cm spot map using a rectangular raster scanning pattern. A spot separation of 2.5 mm was used, and a 5% dose threshold for the ADR calculation was applied. A correction-based calculation algorithm written in Python V3.8 was used for all dose rate distribution calculations.

Our UHDR work to date has used transmission beams where the plateau region of the proton depth dose is used for irradiating samples and detectors. In this region the dose and dose rate do not vary significantly with depth. It is for this reason, and to help with visualisation, that 2D dose rate distributions across a scanned transmission beam are displayed in this manuscript (figure 2).

3. Results

3.1. Beam characterisation

The spot size, σ_x, σ_y, in air at the reference plane is given in figure 3. For a UHDR beam operating at 245 MeV the spot size is $\sigma_x = 4.6$ mm, $\sigma_y = 6.6$ mm.

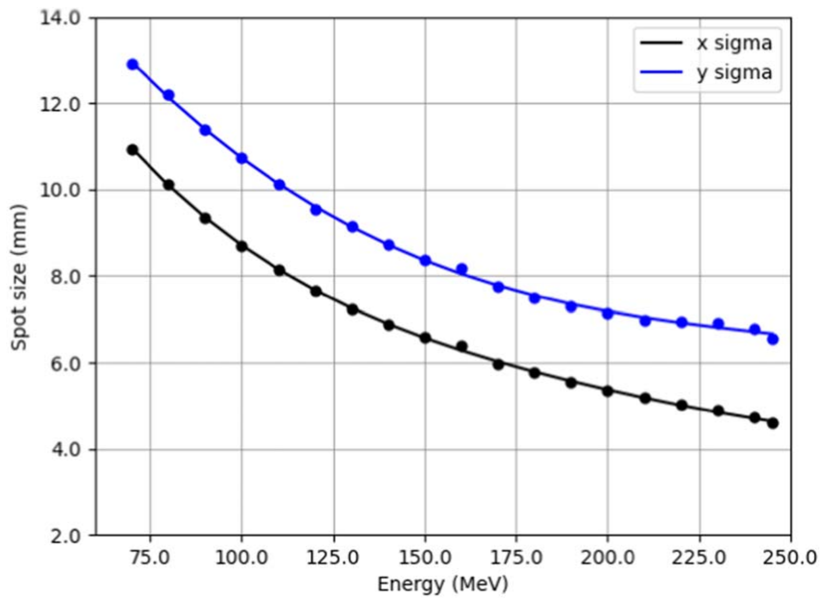

Figure 3. Beam spot size with beam energy measured in air at the reference plane.

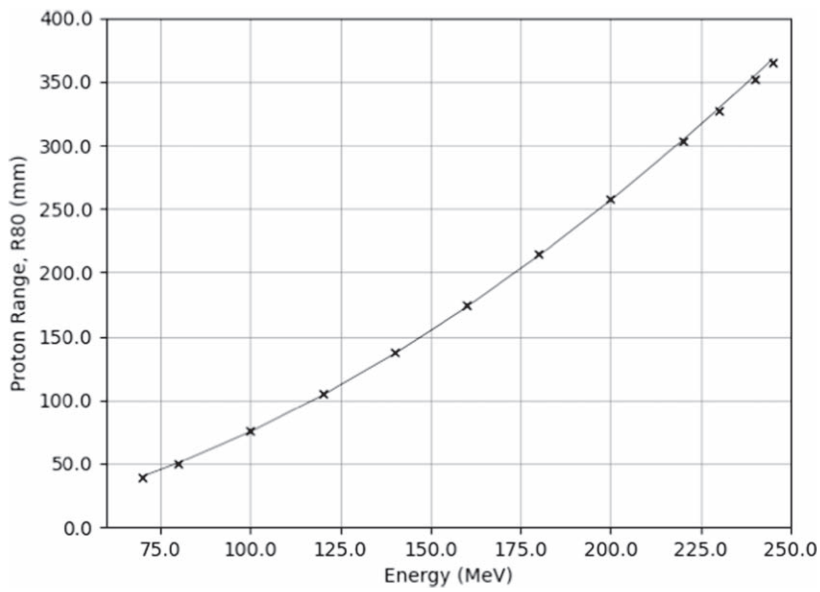

Figure 4. Proton range (R_{80}) in water with cure fitting $R_{80} = 0.00215E^{1.772}$.

Proton range (R_{80}) values are given in figure 4 along with a fitted curve $R_{80} = 0.00215E^{1.772}$ where E is the energy in MeV.

Energy dependent nozzle transmission is shown in figure 5. The transmission at 245 MeV is 7.05 ± 0.10% resulting in a nozzle current of 56.4 ± 0.8 nA. The transmission is within 1% across the range of nozzle currents, from 1.35–56.4 nA.

Relative dose distributions for conventional and UHDR 245 MeV spots are shown in figure 6. The distributions have been normalised to display the dose and dose rate profile for both conventional and UHDR. The spot size (sigma) is comparable within measurement uncertainty between the two dose rate deliveries.

3.2. Absolute dose determination

The current across the monitor chamber electrodes was linear with nozzle current across the full range of dose rates available. When used for beam monitoring the charge is integrated by the IC101 and dead time becomes significant. This IC101 dead time is 55 microseconds in our configuration. Nozzle current dependent MU corrections to account for the dead time are given in figure 7, normalised to 1.0 nA nozzle current (conventional dose rate). For the maximum current that can be requested (56.4 nA nozzle current) the MU correction required is a factor of 0.125 ± 0.015.

The minimum dose to a uniform 10 × 10 cm square field that can be delivered at UHDR has been

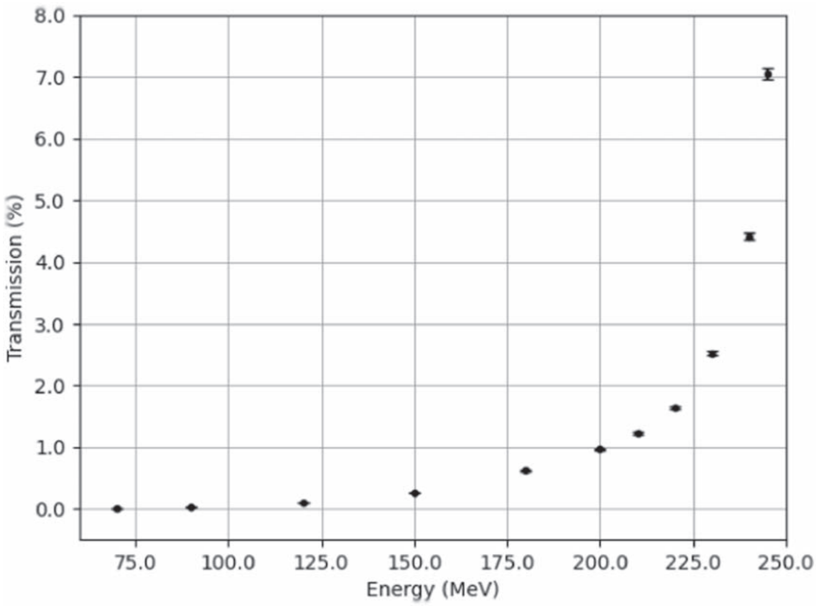

Figure 5. Energy dependent beam transmission from cyclotron to nozzle.

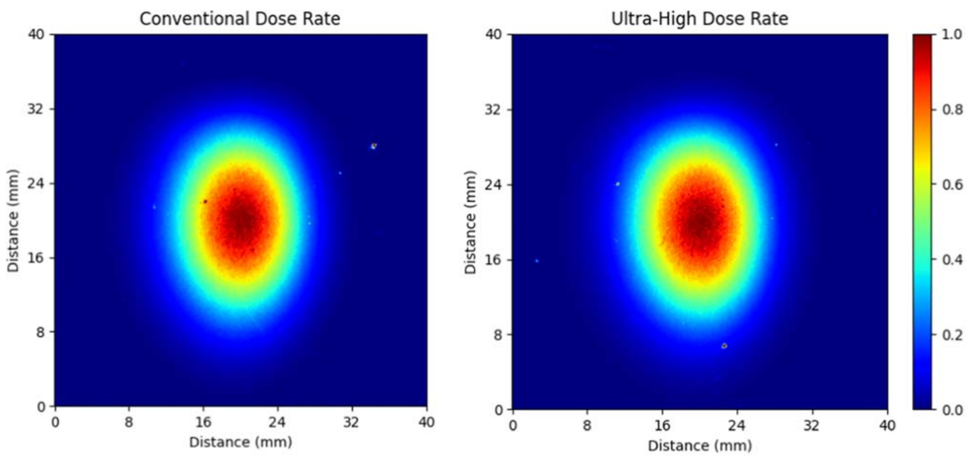

Figure 6. Relative dose and dose rate distribution of a proton spot for conventional (left), and ultra-high dose rates (right) measured at z_{ref}.

measured at z_{ref} as 0.95 ± 0.02 Gy. This lower dose limit is due to the IC101 dead time and beam scanning speed.

The ion recombination correction, k_s, for the Advanced Markus and Roos were 1.011 ± 0.039 and 1.052 ± 0.035 respectively in the UHDR beam. Electrometer saturation was seen in the *Medium* range of the PTW Unidos, and was more significant for small field sizes where the current density across the detector is highest. No electrometer saturation was seen in *High* range, but the resolution of the charge reading is lower.

3.3. Dose rate determination

The instantaneous dose rate to water at 2 cm depth in the centre of a 245 MeV UHDR beam spot is 112.7 Gy s^{-1} and decreases linearly with beam current (figure 8).

Instantaneous depth dose rates along the central axis are given in figure 9 for 70, 150, 230, and 245 MeV. For an individual UHDR spot the highest dose rate is in the plateau region of the depth dose, at 38 mm depth, not in the Bragg peak itself. This is due to lateral scattering off axis (a broader spot) with increasing depth which lower the instantaneous dose rate. For a lower energy beam with shorter depth of penetration, there are fewer scattering events and therefore less scattering off of the central axis of the beam. This results in a dose rate which is greatest in the Bragg peak for low energies.

DADR and ADR distributions for a 245 MeV transmission beam are shown (figure 10) along with a corresponding normalised dose distribution. The DADR is uniform across the central region of the field at. ADR is non-uniform for a rectangular scanning

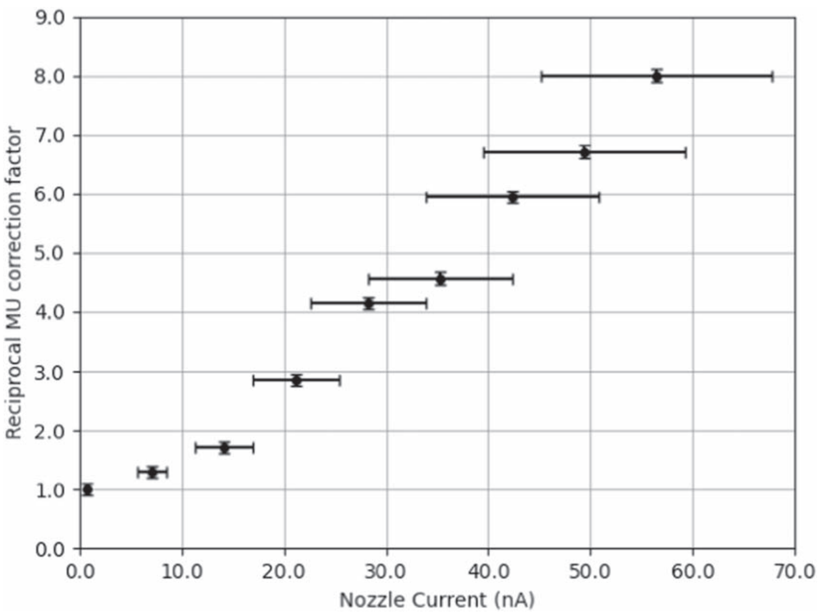

Figure 7. Beam current dependent monitor unit correction factor for a 245 MeV UHDR scanned beam.

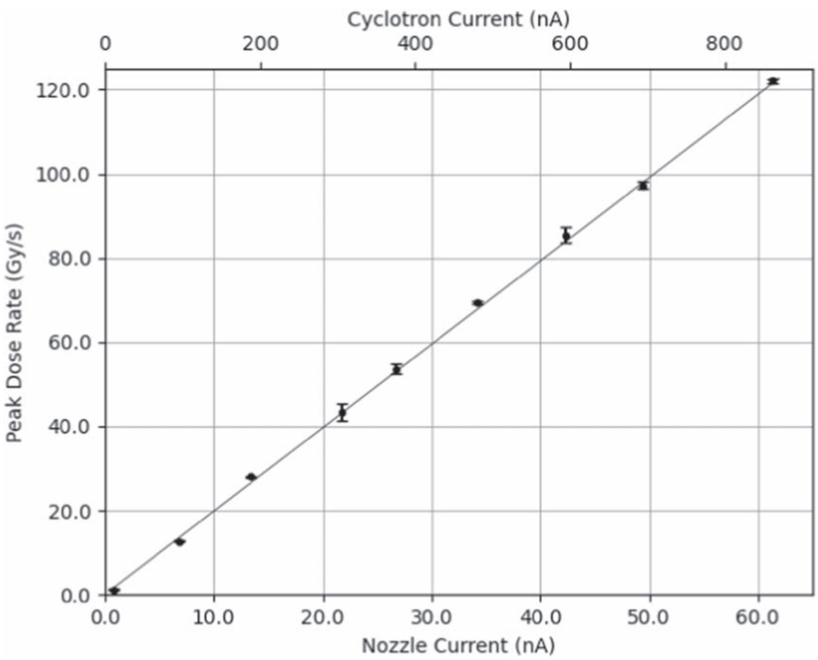

Figure 8. Central axis spot dose rates at Z_{ref} for 245 MeV measured with the PTW microDiamond.

pattern and is in the region 10–15 Gy s^{-1} across the centre of the scanned area for this scanning pattern. This is for a 5 × 5 cm reference field, and significantly higher ADR and DADR can be obtained if an experiment requires by optimising the scanning pattern including scanning a smaller area.

4. Discussion

We have developed an Ultra-High Dose Rate capability with our beamline, predominantly using the plateau region of a 245 MeV beam. Transmission to the nozzle for a beam of this energy is 7.05% resulting in a nozzle current of 56.4 nA for the highest cyclotron current. Spot profiles measured at z_{ref} are comparable for conventional and Ultra-High dose rates with a spot size (sigma) of 4.6 and 6.6 mm in x and y respectively in air at the reference plane. The beam characteristics are maintained at UHDR, and a single beam model can be used for conventional and Ultra-High dose rates.

The current across the integral plane of the monitor chamber electrodes increased linearly with nozzle

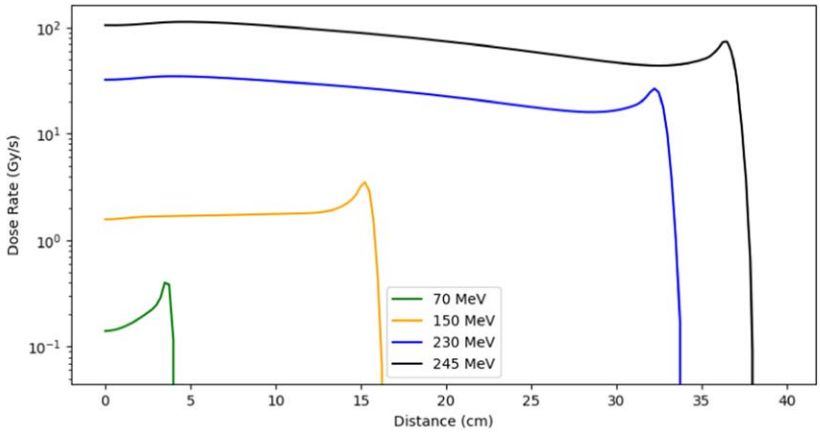

Figure 9. Energy dependent instantaneous dose rates (Gy/s) in water along the central axis of a single proton spot.

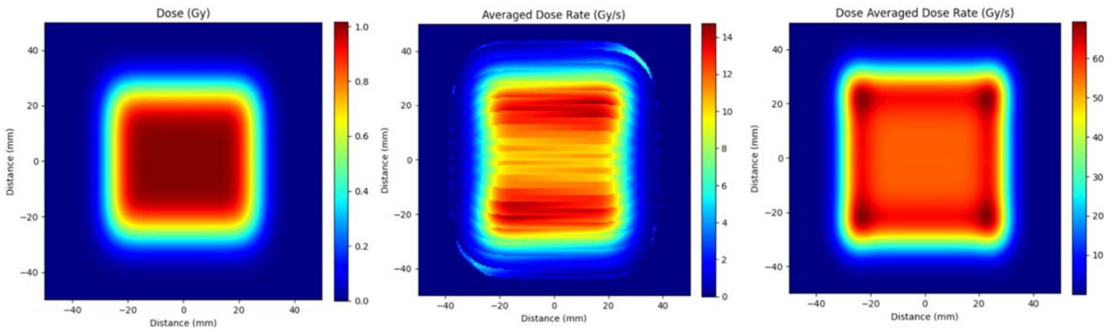

Figure 10. Modelled Dose (left), Averaged Dose Rate (centre), and Dose Averaged Dose Rate (right) distributions for a 245 MeV UHDR transmission beam.

current across the full range of dose rates. This demonstrates that ion recombination in the monitor ion chamber is not significant with this nozzle current density: The UHDR MU correction is only required in our system for the electronic under sampling of the UHDR beam caused by the dead time of the IC101 electrometer.

The MU correction is nozzle current dependent, which can vary during normal operation of the cyclotron. Because of this, a session specific beam monitor calibration is required prior to delivering UHDR beams to increase the dose delivery accuracy. Methods used to reduce the cyclotron current variability (and therefore the dose reproducibility) include carrying out a Smith-Garren calibration prior to carrying out the monitor chamber calibration.

The beam monitor sampling rate of 9.009 kHz results in a minimum spot dwell time of 0.11 ms and therefore a minimum dose to z_{ref} for a 10 × 10 cm field of 0.95 Gy. The dose reproducibility with the existing hardware means a method of dose verification is required when carrying out UHDR irradiations for radiobiology experiments. Dose verification, in our case using EBT3 Gafchromic film, is used to validate the delivered dose for *in-vitro* experiments.

The ion recombination correction for the PTW Advanced Markus at UHDR determined using the two-volt method is 1.011 ± 0.039. This comparable (to within 0.7%) to three other centres with the same accelerator measured at 250 MeV [15]. Comparison of k_s for the Roos and Advanced Markus detectors confirm that the Advanced Markus is a more suitable detector for UHDR (lower correction required) due to the smaller electrode gap.

A peak instantaneous dose rate of 112.7 Gy s^{-1} was measured at z_{ref} in water for a UHDR beam. FLASH experiments with transmission beams carried out at 2–5 cm water equivalent depth are optimal: being beyond the build-up region resulting in a higher dose rate than at the surface, and a suitable depth in water for accurate dose measurement.

We have used beam transmission data to simulate the dose rate for beams across the full energy range of our beamline (from 70–245 MeV), which is designed to be the same characteristics as a clinical ProBeam system. The lowest dose rate along the spot central axis is less than 10 Gy s^{-1} for energies below 230 MeV. This gives an understanding of how system could be used to induce normal tissue sparing using PBS protons, especially when more data is added to the literature on the lower dose rate limit to induce the FLASH effect. Hardware alterations would be required to deliver dose rates of above the order of 10 Gy s^{-1} at less than 200 MeV for a clinical system.

For PBS UHDR transmission beams the dose rate distribution is highly dependent on the scanned field size and dose rate definition used, as has been reported elsewhere [16]. For square PBS areas of greater than 2 cm^2 the ADR is typically less than 40 Gy s^{-1}, however the DADR is greater than this threshold. ADRs of > 40 Gy s^{-1} can be achieved with our system, like all other PBS proton systems, by adjusting the scanning pattern, spot separation, and scan area.

Alternative methods to increase this dose rate further in the future could include increasing the transmission (using a higher energy), increasing the cyclotron current, or modification of beamline hardware and optics to achieve a smaller spot size. Our horizontal research beamline utilises a magnet quadrupole triplet in the final focussing section of the beamline. This quadrupole arrangement has uneven demagnification properties, and thus at the optimal focus produces an elliptical beam spot. Tuning this system to produce a circular beam spot will reduce current density, and thus dose rate. Although the use of an elliptical beamspot in our research line is different to that of the clinical facility, we are not aware of any significant reason why an elliptical beamspot would be detrimental to preclinical research.

Carefully designed PBS experiments can be carried out to investigate the FLASH effect with our system. We plan to update the beam monitoring electronics in the near future to further improve the dose reproducibility when delivering UHDR.

5. Conclusion

The characterisation of Beamline A for use at UHDR has been presented. UHDR irradiations can be carried out using PBS protons at our facility for experimental work investigating UHDR dosimetry and the FLASH effect. The data set out in this publication can be used for designing experiments at this UK research facility.

To our knowledge this is also the first thorough characterisation of UHDR irradiation using the ProBeam cyclotron at energies less than 250 MeV. Our results demonstrate the dose rates achievable across the clinical energy range of the system (70–245 MeV), which is a vital step in understanding the challenges and opportunities when translating proton FLASH into clinical use.

Acknowledgments

This research was funded by the Science and Technology Facilities Council STFC [ST/T506217/1] and supported by Cancer Research UK RadNet Manchester [C1994/A28701], NIHR Manchester Biomedical Research Centre[grant number: BRC-1215-20007], European Union's Horizon 2020 Research and Innovation Programme, INSPIRE [730983], the Engineering and Physical Sciences Research Council [EP/R023220/1], STFC Impact Acceleration Account, and the Christie Charitable Fund.

We thank John Gordon from Pyramid Technical Consultants (Waltham MA, USA) as well as Matt Clarke, David Lines, and Shaun Atherton from The Christie Proton Beam Therapy Centre (Manchester, UK) for their support.

Data availability statement

The data cannot be made publicly available upon publication because no suitable repository exists for hosting data in this field of study. The data that support the findings of this study are available upon reasonable request from the authors.

ORCID iDs

J D Aylward https://orcid.org/0000-0002-0801-228X
S Manger https://orcid.org/0000-0002-4475-2066
J W Warmenhoven https://orcid.org/0000-0002-3638-7759
K J Kirkby https://orcid.org/0000-0002-0901-210X

References

[1] Favaudon V *et al* 2014 Ultrahigh dose-rate FLASH irradiation increases the differential response between normal and tumor tissue in mice *Sci. Transl. Med.* **6** 245ra93

[2] Vozenin M, Hendry J and Cl L 2019 Biological benefits of ultra-high dose rate FLASH radiotherapy:sleeping beauty awoken *Clinical Oncology* **31** 407–15

[3] Esplen N, Mendonca M and Bazalova-Carter M 2020 Physics and biology of ultrahigh dose-rate (FLASH) radiotherapy: a topical review *Phys. Med. Biol.* **65** 23TR03

[4] Ashraf M, Rahman M, Zhang R, Williams B, Gladstone D, Pogue B and Bruza P 2020 Dosimetry for FLASH radiotherapy: a review of tools and the role of radioluminescence and cherenkov emission *Front. Phys.* **8**

[5] Brown K, Carey D, Iselin F and Rothacker F 1980 TRANSPORT: a com-puter program for designing charged-particle beam-transport systems *CERN Yellow Reports: Monographs* (Also publ. as SLAC and FERMILAB)

[6] Beyreuther E, Brand M, Hans S, Hideghéty K, Karsch L, Leßmann E, Schürer M, Szabó E and Pawelke J 2019 Feasibility of proton FLASH effect tested by zebrafish embryo irradiation *Radiother. Oncol* **139** 46–50

[7] Bortfield T and Schlegel W 1996 An analytical approximation of depth-dose distributions for therapeutic proton beams *Phys. Med. Biol.* **41** 1331–9

[8] Bortfeld T 1997 An analytical approximation of the Bragg curve for therapeutic proton beams *Med. Phys.* **24** 2024–33

[9] Patriarca A *et al* 2018 Experimental set-up for FLASH protonirradiation of small animals usinga clinical system *Int J Radiation Oncol Biol Phys* **102** 619–26

[10] Beyreuther E, Baumann M, Enghardt W, Helmbrecht S, Karsch L and Krause M 2018 Research facility for radiobiological studies at the university proton therapy dresden *International Journal of Particle Therapy.* **5** 172–82

[11] International Atomic Energy Agency *et al* 2000 *Absorbed Dose Determination in External Beam Radiotherapy Technical*

Reports Series No. 398 IAEA, Vienna (https://iaea.org/publications/5954/absorbed-dose-determination-in-external-beam-radiotherapy)

[12] Boag J and Currant J 1980 Current collection and ionic recombination in small cylindrical ionization chambers exposed to pulsed radiaiton *Br. J. Radiol.* **53** 471–8

[13] Van de Water S, Safai S, Schippers J, Weber D and Lomax A 2019 Towards FLASH proton therapy: the impact of treatment planning and machine characteristics on achievable dose rates *Acta Oncol.* **58** 1463–9

[14] Folkerts M, Abel E, Busold S, Perez J, Krishnamurthi V and CC L 2020 A framework for defining FLASH dose rate for pencil beam scanning *Med. Phys.* **47** 6396–404

[15] Private correspondance with the Varian FlashForward Consortium dosimetry group

[16] Kang M, Wei S, Choi I, Simone C and Lin H 2021 Quantitative assessment of 3D dose rate for proton pencil beam scanning FLASH radiotherapy and its application for lung hypofractionation treatment planning *Cancers* **13** 3549